Observation of metastable Aβ amyloid protofibrils by atomic force microscopy

James D Harper[1,2], Stanislaus S Wong[3], Charles M Lieber[3] and Peter T Lansbury, Jr[2]

Background: Brain amyloid plaque, a diagnostic feature of Alzheimer's disease (AD), contains an insoluble fibrillar core that is composed primarily of variants of the β-amyloid protein (Aβ). As Aβ amyloid fibrils may initiate neurodegeneration, the inhibition of fibril formation is a possible therapeutic strategy. Very little is known about the early steps of the process, however.

Results: Atomic force microscopy was used to follow amyloid fibril formation *in vitro* by the Aβ variants Aβ1–40 and Aβ1–42. Both variants first form small ordered aggregates that grow slowly and then rapidly disappear, while prototypical amyloid fibrils of two discrete morphologies appear. Aβ1–42 aggregates much more rapidly than Aβ1–40, which is consistent with its connection to early-onset AD. We propose that the metastable intermediate species be called Aβ amyloid protofibrils.

Conclusions: Aβ protofibrils are likely to be intermediates in the *in vitro* assembly of Aβ amyloid fibrils, but their *in vivo* role has yet to be determined. Numerous reports of a nonfibrillar form of Aβ aggregate in the brains of individuals who are predisposed to AD suggest the existence of a precursor form, possibly the protofibril. Thus, stabilization of Aβ protofibrils may be a useful therapeutic strategy.

Addresses: [1]Department of Chemistry, Massachusetts Institute of Technology, Cambridge, MA 02139, USA, [2]Center for Neurologic Diseases, Brigham and Women's Hospital and Harvard Medical School, 221 Longwood Ave.-LMRC, Boston, MA 02115, USA and [3]Department of Chemistry and Chemical Biology, Harvard University, 12 Oxford St. Cambridge, MA 02138, USA.

Correspondence: CM Lieber or PT Lansbury
E-mail: cml@cmliris.harvard.edu
lansbury@cnd.bwh.harvard.edu

Key words: amyloid, atomic force microscopy, protofibril

Received: **23 December 1996**
Accepted: **20 January 1997**

Electronic identifier: **1074-5521-004-00119**

Chemistry & Biology February 1997, 4:119–125

Introduction

Alzheimer's disease (AD) is characterized by the presence of neuritic plaque in the brain. The insoluble core of neuritic plaque contains amyloid fibrils comprising variants of the ~4-kDa β-amyloid protein (Aβ; Fig. 1) [1]. Three lines of evidence suggest that amyloid fibril formation causes neurodegeneration. First, fibrils comprising synthetic Aβ are toxic to neuronal cultures, whereas soluble, presumably monomeric, Aβ and amorphous Aβ aggregates have no activity [2]. Second, insoluble Aβ aggregates of undetermined morphology activate microglia in culture [3]. Finally, transgenic mice overexpressing Aβ and its precursor, APP, develop AD pathology, including amyloid plaques, as well as learning and memory deficits over time (the relative timing of the pathological and behavioral changes has yet to be determined) [4]. These and numerous other studies suggest that the inhibition of amyloid formation would be an excellent therapeutic strategy against AD. But for this to be successful an understanding of the detailed molecular mechanism of Aβ amyloid fibril formation would be extremely useful.

Aβ amyloid fibrillogenesis appears to be rate-limited *in vitro* by the requirement for the formation of an ordered Aβ nucleus [5,6]. Studies of the predominant circulating variant of Aβ, Aβ1–40, and the carboxy-terminally-extended variant Aβ1–42 (Fig. 1) showed that Aβ1–42 nucleated much more rapidly than Aβ1–40 [7]. This observation led to the proposal that early-onset familial AD (FAD) may result from abnormally rapid amyloid formation due to an increase in the ratio of Aβ1–42 to Aβ1–40 [7]. Evidence supporting this proposal has accumulated. For example, the plasma of FAD patients contains a higher ratio of Aβ1–42 to Aβ1–40 than age-matched controls [8]. In addition, cultured cells expressing FAD-mutant forms of either of two proteins (APP or presenilin) overexpress Aβ1–42 [9–11]. Neuropathological studies of FAD patients show a parallel trend [12,13]. Finally, transgenic mice expressing FAD mutations produce higher levels of Aβ1–42 relative to Aβ1–40 than control mice lacking the transgene [4,10,11,14].

The mechanistic model of amyloid formation as a nucleation-dependent polymerization offers a plausible explanation for FAD. However, the details of the *in vitro* mechanism have not been elucidated, due to two significant experimental problems. First, the methods used to measure amyloid, primarily turbidometry and sedimentation, do not necessarily distinguish between fibrillar morphologies, so a single product morphology has been tacitly assumed. Second, these two methods are unable to detect small Aβ oligomers, so the early steps of the assembly process have not been elucidated. Small oligomeric Aβ species have been separated and/or detected by three

Figure 1

H_2N–DAEFRHDSGYEVHHQKLVFFAEDVGSNKGAIIGLMVGGVV–CO_2H
Aβ1–40

H_2N–DAEFRHDSGYEVHHQKLVFFAEDVGSNKGAIIGLMVGGVVIA–CO_2H
Aβ1–42

Sequences of the two Aβ variants Aβ1–40 and Aβ1–42.

methods: analytical ultracentrifugation — Aβ1–40 (at 450 μM) produces a slowly sedimenting species (proposed to contain ~1000 Aβ1–40 molecules), which was observed in addition to the rapidly sedimenting, probably fibrillar, material [15]; gel filtration chromatography — both Aβ1–40 and Aβ1–42 (at 220 μM) were observed to produce a slowly sedimenting species (estimated by gel filtration chromatography to be >100 kDa [16]; and dynamic light scattering — under acidic conditions, an oligomeric Aβ1–40 species, proposed to be a micelle (critical concentration in 0.1 N HCl = 100 μM), was rapidly formed [17]. The methods used are not capable of providing detailed structural information.

Atomic force microscopy (AFM) is an ideal tool to follow the early events of Aβ amyloid fibril assembly because it is capable of directly detecting and measuring the dimensions of small proteinaceous species that are adsorbed from aqueous media (Fig. 2) [18,19]. Previous AFM studies of Aβ amyloid did not follow the process of fibril formation, but focussed on a single time point, after long incubations of concentrated solutions of Aβ1–40 (250 μM) [20]. We chose to follow incubations slightly in excess of the critical concentration for amyloid formation ([Aβ1–40] = 45 μM, [Aβ1–42] = 20 μM) [21], on the grounds that these conditions closely approximate those under which amyloid formation is likely to occur in most types of AD. In addition, multiple time points were analyzed in order to obtain information about the mechanism of fibril formation.

Results

Rapid formation of discrete protofibrils by Aβ1–40

At intervals, Aβ1–40 solutions were gently agitated to evenly suspend any aggregates before aliquots were removed from the otherwise undisturbed solutions and the structural properties of the Aβ species adsorbed onto mica were analyzed by AFM. Small elongated Aβ oligomers, termed 'protofibrils', became visible during the first week of incubation (Fig. 3). The early protofibrils had diameters, inferred from the heights of the topographs (see later) [18,19] of 3.1±0.31 nm and lengths in the range 20–70 nm. As shown in Figures 3 and 4 (green arrows), the protofibrils elongated over three weeks while retaining a constant diameter (the measured heights will be referred to as diameters here, although the cross-section may not

Figure 2

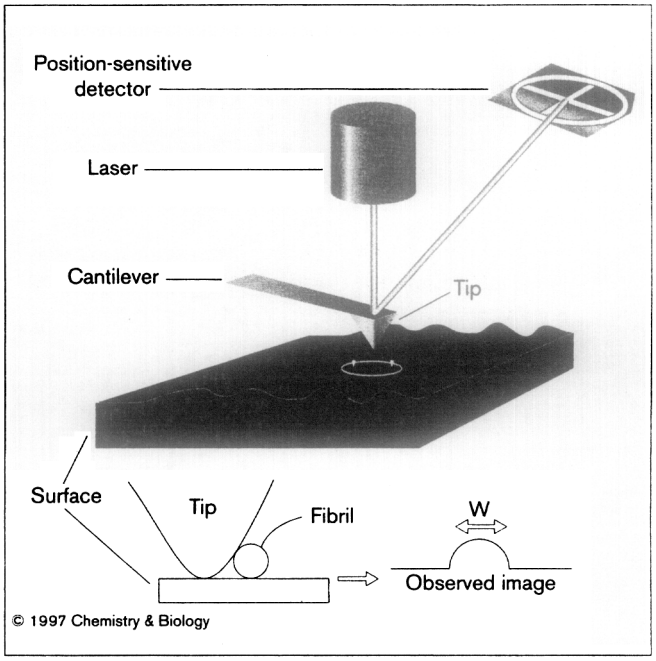

AFM measures the deflection of a sensitive cantilever with a silicon probe tip as a sample adsorbed onto a smooth substrate (e.g. mica) is rastered underneath. The inset shows a schematic of the tip–surface interaction, which demonstrates that the height of an object above the surface can be determined, but that dimension in the plane of the image (W) is difficult to measure accurately, due to the shape and the finite size of the tip. The overestimation of width is related to the height and the true width of the feature and the shape of the 10–20 nm diameter silicon tip, which is difficult to determine accurately [18,19]. It should be noted that the elasticity of the features is important in the measurement of apparent height [18,19]. The upper portion of the diagram is courtesy of Digital Instruments, Santa Barbara, CA.

be circular) reaching lengths often exceeding 100 nm. A parallel incubation at much higher Aβ1–40 concentration (200 μM) developed protofibrils of similar length in two days, and these protofibrils were stable for more than two weeks after dilution to 20 μM (data not shown). The protofibrils often showed small regular variations in diameter with a periodicity of 20±4.7 nm (see green arrow in Figure 4). The small size of these protofibrils preclude their observation by turbidity [7,21].

Formation of type-1 and type-2 fibrils

After four weeks of incubation, long (>1 μm) Aβ1–40 fibrillar species (designated type 1-fibrils) of at least twice the diameter of the protofibril (7.8±0.45 nm) and characterized by a periodic modulation in diameter (period = 43±0.50 nm) appeared (Figs 3,4, red arrows). Strikingly, short (<500 nm) type-1 fibrils were rarely seen. After five weeks, the protofibrils had disappeared completely and a second fibril type (type-2 fibril, diameter = 4.5±0.43 nm) appeared (yellow arrows). Further studies are required in order to determine if the type-2

Figure 3

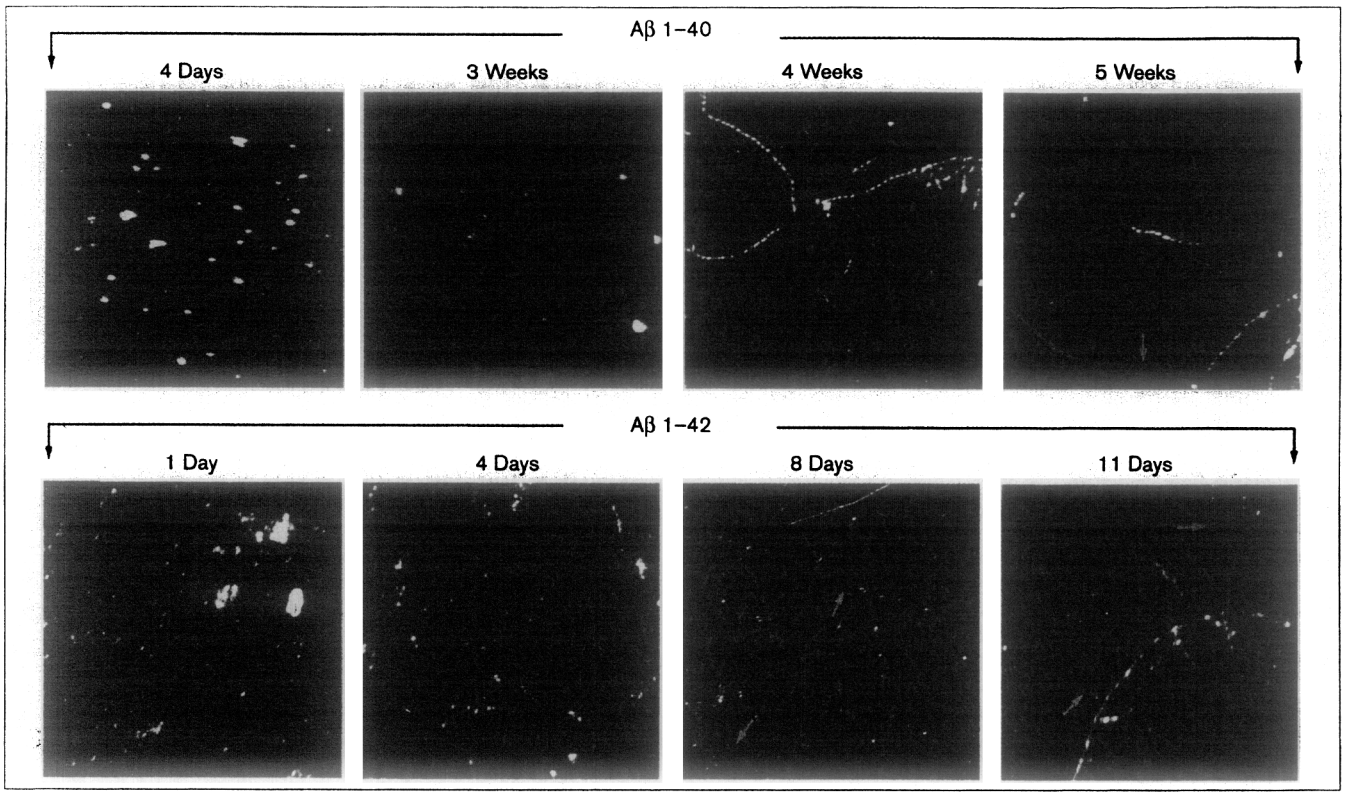

Representative 2 μm square AFM images of the time course of fibril formation by Aβ1–40 (at 45 μM, top row) and Aβ1–42 (at 20 μM, bottom row). In each image, the mica surface appears dark brown, and the brightness of the features increases as a function of their height (for example, the features shown in the 4 day Aβ1–42 image appear brighter than the analogous features in the 3 week Aβ1–40 image because they are higher (*vide infra*); in addition, the very bright features in the early images are probably large amorphous aggregates). For both Aβ1–40 and Aβ1–42, the progression from small protofibrils (green arrows) to longer protofibrils (also green arrows) to fibrils of two types (type 1 = red, type 2 = yellow) is clear, as is the absence of protofibrils at the latest time points. It is also clear that the progression from protofibrils to fibrils occurs more rapidly for Aβ1–42, despite the fact that protein concentration is lower, consistent with the conclusion based on turbidometric methods [7].

fibril, which appears later in the Aβ1–40 incubation, is the thermodynamic product. The diameter of type-1 Aβ1–40 fibrils resembled Aβ1–40 fibrils formed *in vitro* [22] and amyloid fibrils derived from AD brain (width of ~8nm inferred from electron microscope images; D. Selkoe, personal communication).

Rapid assembly of Aβ1–42

Amyloid fibril formation by Aβ1–42 followed a similar, but accelerated, time course to Aβ1–40 [7] despite the fact that the Aβ1–42 concentration was, as it is *in vivo* [8], significantly lower (20 μM) than Aβ1–40 (45 μM). Protofibrils formed within the first day of incubation and elongated over time (Fig. 3). Long (almost always > 1 μm, usually > 5 μm) Aβ1–42 type-1 and type-2 fibrils were detected after 8 days of incubation and all protofibrils had disappeared by 11 days. The observed kinetic differences between Aβ1–42 and Aβ1–40, which are consistent with turbidometric studies, support the proposal that elevated levels of Aβ1–42 lead to more rapid amyloid formation in FAD [7]. This scenario has been supported by numerous studies of the levels of Aβ1–42 and Aβ1–40 in the plasma and brain tissue of FAD patients and in the culture media of cells stably transfected with FAD mutant gene products (see above).

Dimensions of Aβ1–42 and Aβ1–40 oligomers

The measured diameter of the Aβ1–42-derived species differed from the analogous Aβ1–40 species (Fig. 5). The Aβ1–42 protofibrils had a larger diameter (4.2 ± 0.58 nm) than the Aβ1–40 protofibrils, but a similar periodicity (22 ± 3.1 nm). Like Aβ1–40, two types of fibrils were detected; periodic type-1 fibrils (7.3 ± 0.53 nm, ~43 nm period) and type-2 fibrils (3.8 ± 0.43 nm). The difference in diameter between the Aβ1–42 and Aβ1–40 protofibrils could be explained by the fact that the structural subunit β sheet of Aβ1–42 may contain two additional residues [23,24].

Figure 4

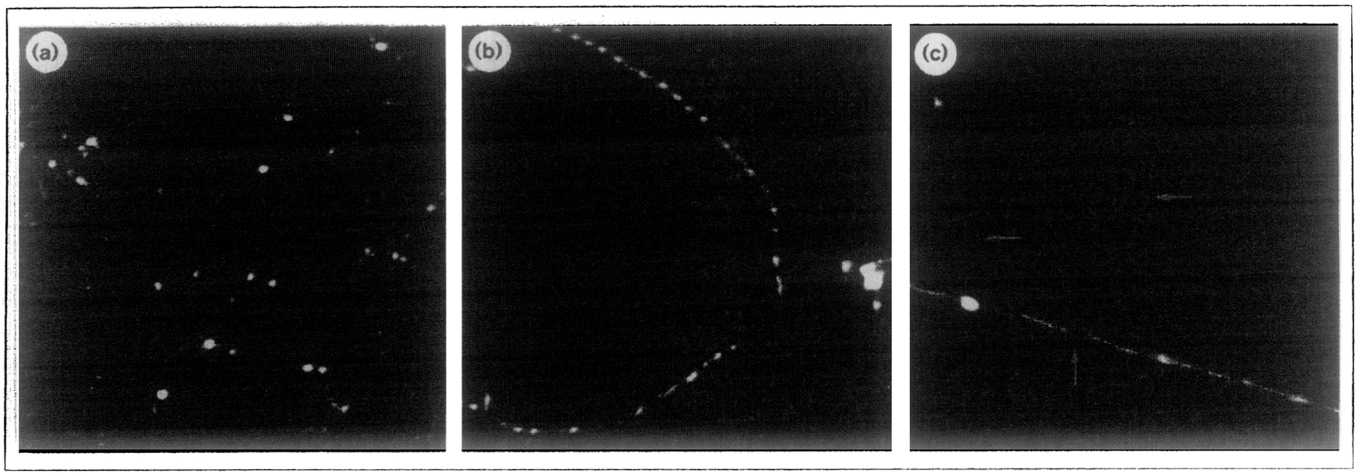

Representative 1 μm square images of three distinct Aβ1–40 aggregate morphologies (Aβ1–42 species have a similar appearance, Fig. 3). Areas of increasing brightness in each image correspond to areas of greater height. The relative height scales of each image were chosen to maximize contrast in the features of interest, so height comparisons between images should not be made. **(a)** A field of protofibrils with green arrows pointing to peaks bordering two clearly defined periodic height modulations (~ 40 nm) along the long axis of the protofibrils. Bright features correspond to crossed protofibrils. **(b)** Type-1 fibrils are indicated (protofibrils can also be seen) with red arrows marking peaks bordering two periods on a type-1 fibril (~ 80 nm). The helical nature of the periodic modulations is clear. **(c)** Type-2 fibrils are clearly distinct from both protofibrils and type-1 fibrils. Although they lack the regular height increases which characterize both protofibrils and type-1 fibrils, they do show less regular discontinuities (yellow arrows) at irregular intervals often >100 nm.

Figure 5

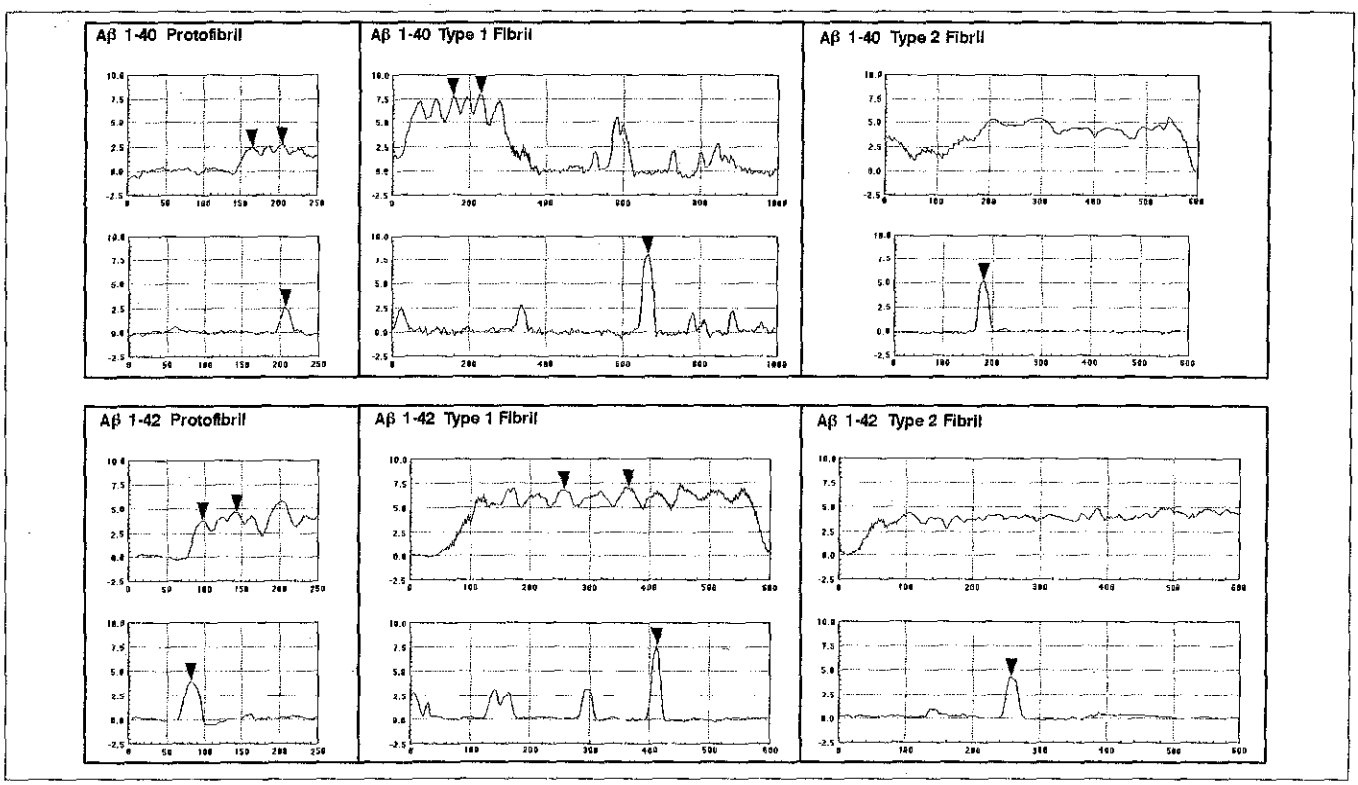

The dimensions of the six distinct species (protofibrils, type-1 fibrils, and type-2 fibrils comprising Aβ1–40 (top) and Aβ1–42 (bottom)). The top row corresponds to the images in Figure 4. In each panel, axial sections are at the top and cross sections at the bottom. Due to the nonlinear nature of these species, axial sections showing more than three repeats are difficult to obtain. Note that the vertical axes are all at the same scale, whereas the horizontal scales vary. Cursors are set to indicate two periods in the axial sections and to show the cross section of the species of interest. Vertical axes for all plots: height (nm). Horizontal axes for all plots: horizontal distance (nm).

Discussion

A scenario in which Aβ protofibrils are intermediates in the assembly of the Aβ-amyloid fibril (Fig. 6) is supported by the fact that the disappearance of protofibrils occurs over a shorter time period than protofibril elongation and is concurrent with the appearance of fibrils. Several additional observations are pertinent to discussions of the probable mechanism. First, protofibril elongation is much slower than fibril elongation. The scarcity of small fibrils suggests that once fibrils are nucleated, their growth is rapid and favorable [6,7]. Second, the diameters of the Aβ1–40 protofibrils and the Aβ1–40 fibrils (both types) are clearly different, which precludes a simple end-to-end protofibril association mechanism. In the case of Aβ1–42, however, the type-2 fibrils (but not the type-1 fibrils) have a similar diameter to the protofibril, so a linear association mechanism can not be ruled out. Third, the existence of an apparent threshold protofibril length before fibrils appear suggests that a minimal overlap between protofibrils may be required to stabilize a structure in which two or more protofibrils wrap around one another. Thus, the fibril diameter may result from two or more protofibrillar subunits, analogous to the transthyretin amyloid fibril [25,26]. Subunit structure has also been seen by electron microscopy of analyzed fibrils comprising unnatural Aβ fragments [27]. Finally, an incubation of Aβ1–40 (45 μM) that was not disturbed for seven weeks, but was otherwise identical to those described above, contained only protofibrils, suggesting that an enhanced frequency of protofibril–protofibril encounters in agitated solutions promotes fibril formation. Although the direct precursor mechanism is attractive, we have not ruled out the possibility that protofibrils are rapidly formed, but are in fast equilibrium with monomeric Aβ, which slowly assembles into the more stable type-1 and type-2 fibrils (Fig. 6). We believe that this is unlikely, although in either scenario the stabilization of protofibrils would inhibit fibril formation, either by blocking protofibril–protofibril interactions or by slowing the protofibril–monomer equilibrium.

Figure 6

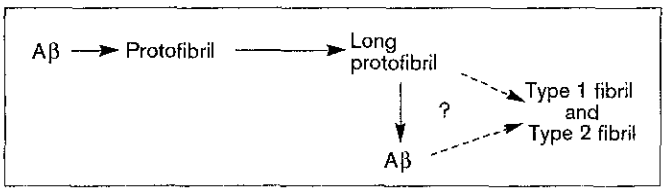

A model for Aβ-fibril assembly, based on the images presented in Figures 3 and 4. Whether the protofibrils are assembly precursors of the fibrils or whether the protofibrils are in fast equilibrium with monomer, which slowly reassembles to type-1 and type-2 fibrils, has not been determined (? in Figure), although suggestive evidence for the former relationship is presented in the text. In addition, it is not clear whether the type-1 or the type-2 fibril, or another species, is the most stable product. It must be emphasized that species which do not absorb onto mica are not seen by this method. However, preliminary experiments using a hydrophobic graphite surface (HOPG) show the same species and no additional ones. In addition, since the velocities of the individual steps may have different concentration-dependencies, it is conceivable that the lifetimes of these species may be altered at lower or higher [Aβ] or that new species become apparent. The protofibril-to-fibril transition seems to be the best candidate for the nucleation-dependent step [6,7], because protofibrils apparently must reach a certain length and/or concentration before rapid fibril growth occurs. Growth of the fibrils, once nucleated, may be first order in [Aβ] [17,31,32].

Although there is no direct evidence presently available for the transient existence of Aβ protofibrils *in vivo*, an apparently nonfibrillar form of deposited Aβ, termed diffuse amyloid plaque, is prevalent in individuals known to be predisposed to AD, leading to the proposal that it represents an innocuous precursor to neuritic amyloid [28]. Diffuse plaque may contain protofibrillar Aβ that is not easily detected by electron microscopy. It will be important to study this material by AFM in the future. Significantly, Aβ protofibrils, like diffuse amyloid plaques, are more difficult to sediment than amyloid fibrils (Dominic Walsh and David Teplow, personal communication).

The conversion of protofibrillar Aβ into fibrillar Aβ may be a critical step in AD pathogenesis. Inhibition of this transition, regardless of whether it is a direct conversion or occurs via the Aβ monomer, would inhibit amyloid formation. ApoE may inhibit this process by binding protofibrils, as suggested by kinetic [21] and biochemical studies [29]. This may explain the correlation between apoE genotype and AD susceptibility/age of onset [30]. It may be possible to find an exogenous compound that similarly blocks the protofibril-to-fibril transition. This would be a practical mode of inhibition, since the inhibitor could be effective in low concentrations relative to Aβ. If, as suggested by *in vitro* studies of neurotoxicity and microglia activation [2,3], the Aβ amyloid fibril is responsible for initiating AD neurodegeneration, then the Aβ protofibril should be targeted by drug discovery efforts aimed at developing a therapeutic for AD.

Significance

The presence of amyloid fibrils, ordered protein aggregates comprising Aβ protein variants, in the brain is a defining and unique feature of Alzheimer's disease (AD). Because it is very difficult to reconstruct the *in vivo* pathway based on neuropathological data, we study the *in vitro* mechanism of Aβ amyloid formation, on the assumption that it may be analogous to the situation in AD. In this study, amyloid formation by the two predominant Aβ variants was followed using atomic force microscopy (AFM), a relatively new technique which allows one to create a nanometer-scale image by physically contacting species adsorbed to a smooth surface. In both cases, the first-formed species was not the expected amyloid fibril, but a smaller species of discrete morphology. This species slowly elongated, then rapidly

disappeared in favor of typical amyloid fibrils. We propose to call this metastable intermediate the Aβ amyloid protofibril, to indicate the possibility that it represents a fibril assembly intermediate. The overall process was much more rapid in the case of the 42 amino-acid variant Aβ1–42 when compared with the truncated variant Aβ1–40, which is the major circulating species, consistent with the fact that increased expression of the former variant is associated with early-onset AD.

The existence of a metastable intermediate protofibril offers a possible morphological explanation for the commonly observed diffuse amyloid plaque, an apparently innocuous and nonfibrillar form of deposited Aβ which characterizes the brains of individuals who are predisposed to AD. In addition, it suggests a potential therapeutic target, since converging evidence suggests that amyloid fibrils may initiate a cascade of events which culminate in neuronal death. Stabilization of the protofibril intermediate could inhibit fibril formation, thus delaying the onset of neurodegeneration. Finally, there may be endogenous proteins (e.g. apoE) which act in a similar way; these could be protective factors against AD.

Materials and methods

Materials

Synthetic Aβ1–40 was purchased from Quality Controlled Biochemicals Inc. (Hopkinton, MA). Synthetic Aβ1–42 was provided by David Teplow of the Center for Neurologic Diseases.

In vitro *fibril formation and sample preparation*

Stock solutions of Aβ1–40 and Aβ1–42 were made by dissolving each peptide in dimethyl sulfoxide (DMSO) at 0.34 mM (Aβ1–42) or 0.84 mM (Aβ1–40) and, in the case of Aβ1–40, filtering through Millex-FG 0.22 μm filters (Millipore). Final concentrations of the DMSO stocks were determined by quantitative amino acid analysis. Aliquots of the DMSO stock solutions (9 nmol in ~ 11 μl for Aβ1–40, 4 nmol in ~ 11 μl for Aβ1–42) were added to aqueous buffer (200 μl total volume, 100 mM NaCl, 10 mM NaH_2PO_4, pH 7.4) and immediately vortexed to mix before allowing fibril formation to proceed at room temperature.

Atomic force microscopy

At intervals, otherwise undisturbed aggregation mixtures were mixed by gentle tapping and samples were prepared for imaging by transferring 5 μl of the suspension to the surface of freshly cleaved mica (Ted Pella Inc., Redding, CA). After 1 min the remaining suspension was removed by absorption and the substrate was rinsed twice with 50 μl water to remove salt and loosely bound peptide. Excess water was removed with a gentle stream of filtered compressed air and the sample was imaged immediately. All images were obtained under ambient conditions with a Nanoscope IIIa MultiMode scanning probe workstation (Digital Instruments, Santa Barbara, CA) operating in TappingMode™ using 120 μm etched silicon NanoProbes™ (125 μm cantilever, spring constant = 20–100 $N m^{-1}$, tip radius ≈ 5–10 nm) (Probe Model TESP, Digital Instruments). Scanning parameters varied with individual tips and samples, but typical ranges were as follows: starting RMS amplitude, 2.0 V; setpoint, 1.5–1.75 V; tapping frequency, 250–350 kHz; scan rate, 0.5–2 Hz. The diameters of features as described here were obtained by averaging 30 peak height values obtained for the stated morphology using nanoscope section analysis software (± standard deviation). Periodicities were determined by averaging 30 peak-to-peak distances (± standard deviation) except for the case of the Aβ1–42 type 1 fibril, where only 12 values were available.

Acknowledgements

This work was funded by a grant from the National Institutes of Health (to P.L.). Funds for the purchase of the AFM were provided by the Foundation for Neurologic Diseases (Newburyport, MA). We thank Dennis Selkoe for his support and for his comments on the manuscript. J.H. was a National Institutes of Health biotechnology graduate trainee. S.W. thanks the Fonds pour la Formation de Chercheurs et l'Aide a la Recherche (Quebec, Canada) for financial support. We are also grateful for the intellectual input of David Teplow and Dominic Walsh of the Center for Neurologic Diseases, who shared their results with us prior to publication.

References

1. Selkoe, D. (1995). Deciphering Alzheimer's disease: molecular genetics and cell biology yield major clues. *J. NIH Research* **7**, 57–64.
2. Lorenzo, A. & Yankner, B.A. (1994). β amyloid neurotoxicity requires fibril formation and is inhibited by Congo red. *Proc. Natl Acad. Sci. USA* **91** 12243–12247.
3. El Khoury, J., Hickman, S.E., Thomas, C.A., Cao, L., Silverstein, S.C. & Lokie, J.D. (1996). Scavenger receptor-mediated adhesion of microglia to β-amyloid fibrils. *Nature* **382**, 716–719.
4. Hsiao, K., *et al.*, & Cole, G. (1996). Correlative memory defects, Aβ elevation, and amyloid plaques in transgenic mice. *Science* **274**, 99–102.
5. Lansbury, P.T., Jr (1996). A reductionist view of Alzheimer's disease. *Acc. Chem. Res.* **29**, 317–321.
6. Jarrett, J.T. & Lansbury P.T., Jr (1993). Seeding the 'one-dimensional crystallization' of amyloid: a pathogenic mechanism in Alzheimer's disease and scrapie? *Cell* **73**, 1055–1058.
7. Jarrett, J.T., Berger, E.P. & Lansbury P.T., Jr (1993). The carboxy terminus of β amyloid protein is critical for the seeding of amyloid formation: implications for the pathogenesis of Alzheimer's disease. *Biochemistry* **32**, 4693–4697.
8. Schneuner, D., *et al.*, & Younkin, S.G. (1996). Secreted amyloid β-protein similar to that in the senile plaques of Alzheimer's disease is increased *in vivo* by the presenilin 1 and 2 and APP mutations linked to familial Alzheimer's disease. *Nat. Med.* **2**, 864–870.
9. Suzuki, N., *et al.*, & Younkin, S.G. (1994). An increased percentage of long amyloid β protein secreted by familial amyloid β protein precursor (bAPP717) mutants. *Science* **264**, 1336–1340.
10. Borchelt, D.R. *et al.*, & Sisodia, S.S. (1996). Familial Alzheimer's disease-linked presenilin 1 variants elevate Aβ1–42/Aβ1–40 ratio *in vitro* and *in vivo*. *Neuron* **17**, 1005–1013.
11. Citron, M., *et al.*, & Selkoe, D.J. (1997). Mutant presenilins of Alzheimer's disease increase production of 42-residue amyloid β protein in both transfected cells and transgenic mice. *Nat. Med.* **3**, 1–6.
12. Iwatsubo, T., Odaka, A., Suzuki, N., Mizusawa, H., Nulina, N. & Ihara, Y. (1994). Visualization of Aβ42(43) and Aβ40 in senile plaques with end-specific Aβ monoclonals: evidence that an initially deposited species is Aβ42(43). *Neuron* **13**, 45–53.
13. Lemere, C., *et al.*, & Arango, J.C. (1996). The E280A presenilin 1 mutation leads to a distinct Alzheimer's disease phenotype: increased Aβ42 deposition and severe cerebellar pathology. *Nat. Med.* **2**, 1146–1150.
14. Duff, K., *et al.*, & Younkin, S.G. (1996). Increased amyloid β42(43) in brains of mice expressing mutant presenilin 1. *Nature* **383**, 710–713.
15. Snyder, S.W., *et al.*, & Holzman, T.F. (1994). amyloid β aggregation: selective inhibition of aggregation in mixtures of amyloid with different chain lengths. *Biophys. J.* **67**, 1216–1228.
16. Soreghan, B., Kosmoski, J. & Glabe, C. (1994). Surfactant properties of Alzheimer's Aβ peptides and the mechanism of amyloid aggregation. *J. Biol. Chem.* **269**, 28551–28554.
17. Lomakin, A., Chung, D.S., Benedek, G.B., Kirschner, D.A. & Teplow, D.B. (1996). On the nucleation and growth of amyloid β-protein fibrils: detection of nuclei and quantitation of rate constants. *Proc. Natl Acad. Sci. USA* **93**, 1125–1129.
18. Drake, B., *et al.*, & Hansma, P.K. (1989). Imaging crystals, polymers, and processes in water with the atomic force microscope. *Science* **243**, 1586–1589.
19. Bustamante, C. & Keller, D. (1995). Scanning force microscopy in biology. *Physics Today* **48**, 32–38.
20. Stine, W.B., *et al.*, & Krafft, G.A. (1996). The nanometer-scale structure of amyloid β visualized by atomic force microscopy. *J. Prot. Chem.* **15**, 193–203.
21. Evans, K.C., Berger, E.P., Cho, C.-G., Weisgraber, K.H. & Lansbury, P.T., Jr (1995). Apolipoprotein E is a kinetic, but not a thermodynamic inhibitor of amyloid formation: implications for the pathogenesis and treatment of Alzheimer's disease. *Proc. Natl Acad. Sci. USA* **92**, 763–767.

22. Fraser, P.E., Duffy, L.K., Nguyen, J., Inouye, H. & Kirschner, D.A. (1991). Morphology and antibody recognition of synthetic β-amyloid peptides. *J. Neurosci. Res.* **28**, 474–485.
23. Lansbury, P.T., Jr, *et al.*, & Griffin, R.G. (1995). Structural model of the β amyloid fibril: interstrand alignment of an antiparallel β sheet comprising a C-terminal peptide. *Nat. Struct. Biol.* **2**, 990–998.
24. Halverson, K., Fraser, P.E., Kirschner, D. A. & Lansbury, P.T., Jr (1990). Molecular determinants of amyloid deposition in Alzheimer's disease: conformational studies of synthetic β-protein fragments. *Biochemistry* **29**, 2639–2644.
25. Blake, C.C.F. & Serpell, L. (1996). Synchrotron X-ray studies suggest that the core of the transthyretin amyloid fibril is a continuous β-sheet helix. *Structure* **4**, 989–998.
26. Serpell, L.C., *et al.*, & Blake, C.C.F. (1995). Examination of the structure of the transthyretin amyloid fibril by image reconstruction from electron micrographs. *J .Mol. Biol.* **254**, 113–118.
27 Fraser, P.E., Nguyen, J.T., Surewicz, W.K. & Kirschner, D.A. (1991). pH-dependent structural transitions of Alzheimer amyloid peptides. *Biophys. J.* **60**, 1190–1201.
28. Selkoe, D.J. (1994). Normal and abnormal biology of the β-amyloid precursor protein. *Annu. Rev. Neurosci.* **17**, 489–517.
29. Chan, W., Fornwald, M., Brawner, M. & Wetzel, R. (1996). Native complex formation between apolipoprotein E isoforms and the Alzheimer's disease peptide Aβ. *Biochemistry* **35**, 7123–7130.
30. Corder, E.H., *et al.*, & Perciak-Vance, M.A. (1993). Gene dose of apolipoprotein E type 4 allele and the risk of Alzheimer's disease in late onset families. *Science* **261**, 921–923.
31. Maggio, J.E., *et al.*, & Mantyh, P.W. (1992). Reversible *in vitro* growth of Alzheimer disease β-amyloid plaques by deposition of labeled amyloid peptide. *Prod. Nat. Acad. Sci. USA* **89**, 5462–5466.
32. Naiki, H. & K. Nakakuki. (1996). First-order kinetic model of Alzheimer's β-amyloid fibril extension *in vitro*. *Lab. Invest.* **74**, 374–383.